2012

Evaluation of shoreline change using optical satellite images, case study of Progreso, Yucatan

Garcia-Rubio, Gabriela

http://hdl.handle.net/10026.1/921

http://dx.doi.org/10.24382/4765
University of Plymouth

SHORELINE IDENTFICATION USING SATELLITE IMAGES

Gabriela García-Rubio[1], David Huntley[2], Kenneth Kingston[3], Luciana Esteves.[4]

Abstract

Shoreline identification using satellite images is compared with in situ shoreline measurements in the Yucatan Peninsula to evaluate its potential for studying shoreline changes in places with a paucity of data. This study firstly tests the detection limits of shoreline identification by comparing a SPOT image with ground shoreline measurements, and secondly we show examples of overlaying satellite-derived shorelines from three different years to assess the ability of the technique to quantify real shoreline changes. The mean (-0.19 m) and the standard deviation (4 m) between the ground and satellite-derived shoreline are much smaller than the pixel size. Shoreline changes of more than 30 m were measured between images spanning several years (2004, 2006 and 2008) in areas near to coastal structures and near urban areas without coastal vegetation.

Key words: shoreline identification, satellite images, erosion, beach dynamics, shoreline change, Yucatan, Mexico.

1. Introduction

The coasts of the Yucatan Peninsula show shoreline erosion over the last 15 years according to local observations (Alvarez-Rubio & Ricalde, 2007) but a shoreline change monitoring program or systematic wave measurements does not exist, and only recently some beach profile monitoring has begun on a systematic basis at some beach locations. The analysis of these beach profiles reveals shoreline retreat of more than 20 m after storm events. However regular shoreline monitoring is still missing for most of the Yucatan beaches, severely limiting the ability to assess long term trends in shoreline evolution.

Satellite imagery has become a worth-while tool that may be used to quantify changes in shoreline position over large areas with little or no field measurements. It also has the potential to investigate nearshore dynamics and to update maps frequently (Dinesh Kumar *et al*, 2007; Chu *et al*, 2006; Lafon *et al*, 2004; White & El Asmar, 1999; De Wolf, 1994). There are a number of available sources of satellite optical images that can potentially be used to assess shoreline changes such as SPOT, Landsat TM, ETM+, IRS, IKONOS, with spatial resolutions varying from 30 m to less than 1 m.

There are several methods for identifying the shoreline from optical images, based on clustering techniques, edge detection methods or segmentation procedures using the reflectance values from water and land at specific wavelengths in the electromagnetic spectrum (Addo, Walkden & Mills, 2008; Dinesh Kumar et al, 2007; Liu & Jezek, 2004; Provost et al, 2004; White & Asmar, 1999). To identify the shoreline, reflectance values from the red and the near infrared wavelengths in particular provide useful information.

This study firstly tests the detection limits of shoreline identification from satellite images by comparing in situ data and a satellite image taken within a few days of each other and secondly compares shoreline

[1]School of Earth, Ocean and Environmental Studies, University of Plymouth, Plymouth, UK, 44 1752264715, gabriela.garciarubio@plymouth.ac.uk
[2]School of Earth, Ocean and Environmental Studies, University of Plymouth, Plymouth, UK, 44 1752 584592, D.Huntley@plymouth.ac.uk
[3]School of Earth, Ocean and Environmental Studies, University of Plymouth, Plymouth, UK. 44 1752 584720, K.Kingston@plymouth.ac.uk
[4]School of Geography, University of Plymouth, Plymouth, UK, 44 1752 585971, luciana.esteves@plymouth.ac.uk

position from images of three dates (15th of November 2004, 6th of February 2006 and 20th of September 2008) to assess the ability of satellite-derived shorelines to monitor shoreline changes.

2. Physical setting

This study is focused on the beaches at Progreso on the Yucatan Peninsula, in the SE part of Mexico between the Caribbean Sea and the Gulf of Mexico. Progreso village is a summer destination for local tourists and also is a stop for Caribbean cruises. Along the beach there are mainly summer houses located around 20 m landwards from the High Water Line (HWL). The removal of coastal dunes and coastal vegetation is commonplace in order to build as closely as possible to the sea.

According to some observations erosion has increased in the last 15 years, with considerable erosion rates in the last few years (Alvarez, Rubio & Ricalde, 2007; Solís-Pimentel & Río, 2008). It is stated by local people that 20 years ago, the Yucatan beaches were wide enough to hold a baseball game, whereas currently the beach width ranges from 54 m to as little as 3 m (POETCY, in press). The narrowing of the beaches might be linked to the effect of coastal structures. Modification of the beaches started to intensify during the 1950s, when the construction of summer houses was extended to nearby villages. In 1947 a 2 km long concrete pier was built, which is now extended to 8 km. In 1985, 75 % of the houses to the west of the pier were less than 20 m landwards from the HWL (Meyer-Arendt, 1993). In the 1980s groyne construction became common to protect individual properties from erosion. This practice increased the erosion problems, resulting in the banning of groyne construction by 1985. Although many of the groynes have been removed, some illegal ones still exist and the erosion problems persist.

The study area has typically low wave heights (Hs < 30 cm) and a small tidal range (< 1m), with a mixed regime, with predominance of a diurnal form. The incident waves show two main directions: North and East (Capurro-Filograsso *et al*, 2006). Yucatan beaches have their origin in bioclastic sediments showing low settling velocity due to their flat and angular shape and lower density. Although the mean grain size is 0.55 mm, the grain size varies considerably throughout the year. From March to September coarser grain sizes (0.5-1 mm) are found in the intertidal zone, with a larger cross-shore variation in grain size, while finer grain sizes (0.35 to 0.7 mm) and less cross-shore variation occur from November to March (Capurro-Filograsso *et al*, 2006). Although sediment dynamics have not yet been studied in the area, it is expected that these differences in the grain size and shape will affect the movement and the behaviour of littoral transport (Dyer, 1986).

The yearly frequency of hurricanes in the study area is highly variable. Statistics on tropical storms and hurricanes since 1944-2002 suggest on average a yearly occurrence of 10 tropical systems and hurricanes, of which 3 would be greater than category 3 on the Saffir-Simpson scale (winds between 178 to 209 km/h), 6 of them would be defined as hurricanes (winds of at least 119 km/h), and 4 would be named tropical storms (winds of at least 63 km/h).

These storm frequency and sediment characteristics make the region a dynamic beach environment, in spite of the average low energy conditions. According to beach profiles analysed by Magaña-Chuc (2006) storms and hurricanes can cause more than 10 m of landward migration in the shoreline position as a result of wave heights of only 1m. This suggests that large amounts of energy are not required to create significant shoreline change, undoubtedly in part due to the angular, low density and concave shape of the beach sediments.

3. Methods

3.1 Waterline measurement

In situ waterline measurement was carried out along a stretch of coastline at Progreso in September 2008 using a DGPS. The geographic projection used was the Universal Transverse Mercator, for the 16th North zone. The reference geoid is WGS84. The data have been corrected with a reference point from the Ministry of Geography in Mexico and the resulting accuracy of the measurements is therefore expected to be within 10 cm.

The base station was established at the centre of the area being covered. The mobile station was carried on a golf bag carrier, with the antenna fixed in a vertical position. The waterline measurement was carried out on September 9th 2008 starting at 11:45 local time and ending at 15:39. When measurements started the predicted tide level was 9 cm above the local reference level (BMI) and at the end it was 10 cm below BMI.

An 8 km stretch of coastline was measured by walking with the mobile station along the run up maximum, with data points taken every 3 seconds, at an equivalent alongshore spacing of around 4 metres. On the way back along the same stretch of shoreline, half of the measurements were made following a track near the top of the beach, in order to gain an estimate of the beach width. In total 4,171 points were acquired, 1,359 from the onward journey and the remainder on the return.

3.2 Image analysis

3.2.1 Description of images

The satellite images obtained from the SPOT satellites have a 2A processing level and a J spectral mode. Three images, from 2004, 2006 and 2008 years are considered here. The images have two spectral bands from the visible range and two from the infrared range. Table 1 shows the wavelength range of each band. The time and the predicted tide level for each image are shown in Table 2.

Table 1. Wavelengths detected by each band from the SPOT satellite.

Band No	Wavelength (μm)	Colour
1	0.50 - 0.59	Green
2	0.61 - 0.68	Red
3	0.78 - 0.89	Near Infrared
4	1.58 to 1.75	Mid Infrared

Table 2. Tide levels relative to BMI for each SPOT image used to extract shoreline and the measured slope from beach profiles and their dates.

Date	Local time	Predicted tide (m)	Beach profiles dates	Beach slope
20 Sept 2008	10:17	-0.09	--	--
6 Feb 2006	10:29	0.26	10 Jan 2006	0.15
15 Nov 2004	10:49	-0.29	18 Nov 2004	0.16

3.2.2 Geometric correction

For shoreline identification purposes the precision of spatial location is very important, especially when different images are compared with each other (White & El Asmar, 1999). Therefore geometric correction was carried out using true ground control points (GCP) of main road intersections and streets identified in the image. For each image at least 15 GCPs have been fitted to a 1st order polynomial function and the resulting rms errors are less than 5 m or half of the pixel size.

3.2.3 Shoreline extraction

Before performing shoreline extraction, a mask is used to remove pixels which are not located near the coast and do not provide important statistical information for the shoreline extraction.

The intensities in bands 2 and 3 have been used as input to an unsupervised classification. In a physical sense, as light penetrates the water surface, wavelengths from the red range of the electromagnetic spectrum are attenuated more rapidly than those from the blue range (Morel, 1974). Therefore, red and near infrared are more sensitive to water. Lafon *et al* (2002) show that the near infrared band penetrates to 0.3 m depth, whereas the red and green bands penetrate up to 15 m depth.

In the unsupervised classification, an isodata algorithm is used, which is similar to the k-Means algorithm (Theodoridis & Koutroumbas, 2006). The spectral data is classified into clusters or groups, the number of clusters being specified to initialize the algorithm. In our analysis we specify two clusters, to distinguish between land and water.

The optimum locations of clusters will depend on the image statistics. Each image has different reflectance values and will therefore have different values of spectral intensity at the cluster centres. In Erdas Imagine the algorithm assigns each pixel to the nearest cluster mean. The means of the clusters are then shifted, and the new cluster means are used for the next iteration. The user specifies a convergence threshold as the maximum percentage of pixels whose cluster assignments will remain unchanged between iterations. The classification process will finish when the specified threshold is satisfied.

The result of the process is a classified image in raster format, with two clusters: land and water. To identify the shoreline a line is more appropriate than a series of pixels; therefore ArcGIS is used to transform the image from raster to a vector. The algorithm converts the class boundaries into lines. The line follows the junction of the two pixel classes, removing pixel corners.

After the classification process a visual examination was undertaken; 4 % of the shoreline length was edited manually for the 2004 image and the other images did not require editing.

3.2.4 Satellite-derived shoreline and Ground shoreline

In order to assess the accuracy of the satellite-derived shoreline identification, the near distance algorithm from ArcGIS was used to calculate the nearest distance between the DGPS measurements and the satellite-derived shoreline. The algorithm stored the distance and its angle of measurement. Positive angles mean that the satellite-derived shoreline is seawards relative to the ground shoreline and negative values mean that the satellite-derived shoreline is landwards from the ground shoreline. These shoreline positions have been compared with the shoreline locations on 10 profiles measured on January 10th 2006 and November 18th 2004 (Ismael Mariño – personal communication).

4. Results

4.1 Shoreline identification

The classification process worked very well for the analysed images, even for beach stretches with inlets, ports, groynes and piers. The classification provides a good visual agreement with the satellite image.

The reflectance values from red, green and near infrared wavelengths show a more limited variation and smaller spectral intensities over the water than over the land, as shown in the examples in Figure 1. The smallest values, around 50 to 100, correspond to water, and the higher values, around 150-250, belong to land. The shoreline has been identified as the boundary between the groups, at 70 m in the cases shown in Figure 1A-B. The sharpness of the change in intensities from sea to land means that the shoreline can be identified with an accuracy of a pixel, and this has been confirmed by tests which show that shoreline location is insensitive to the convergence threshold used in the clustering algorithm.

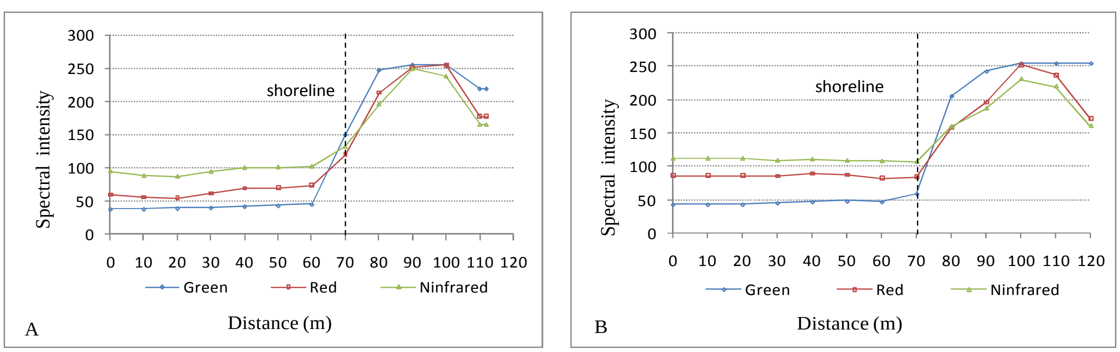

Figure 1. Spectral profiles on cross shore sections between shallow water and land showing the spectral intensities from the three bands (Green, Red, Near Infrared) for locations where the largest offset between the ground and satellite-derived shoreline occurs (A) and where the offset is less than 0.5 m (B).

The visual examination after the classification process showed that the identified shoreline is generally in excellent visual agreement with all the images. The exception was a stretch of shoreline in the 2004 image where very shallow sub-aqueous features caused the apparent shoreline to be placed seaward of the correct location. In this case manual editing was required to ensure that this stretch of beach used a similar cluster classification to the other stretches.

4.2 Satellite-derived shoreline and ground shoreline comparisons.

Over the 8 km shoreline stretch measured, the ground shoreline and the satellite-derived shoreline differ from each other by a mean of -0.19 m and a standard deviation of 4 m. The mean and the standard variation are much smaller than the pixel size, showing that in fact the satellite-derived shoreline is close to the edge of the run up maximum. Figure 2 shows an example of the fitting of both shorelines. The agreement over most of the beach stretch is well within the pixel size.

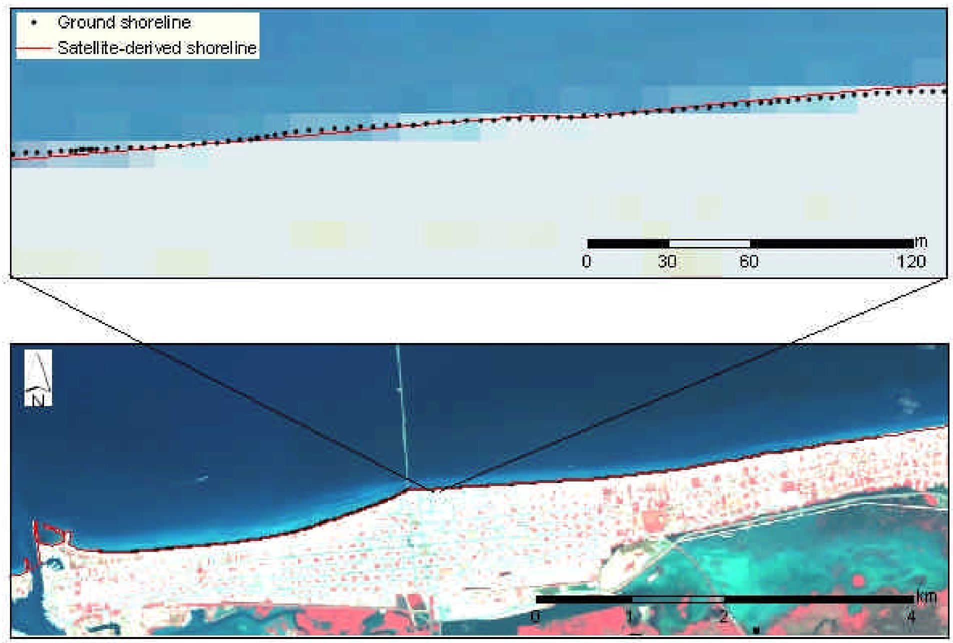

Figure 2. Ground shoreline and satellite-derived shoreline superimposed on the image from 20th of September 2008. The upper image shows close up from the lower image. The black dots represent the ground shoreline and the red line the satellite-derived shoreline.

Physically this comparison suggests that the satellite is classifying very shallow water as water and dry sand as land, and even though there is a variation in the boundary position, this variation remains within the pixel size. This intercomparison therefore bodes well for future attempts to detect real changes of shoreline location of larger magnitude than the pixel resolution (10 m). Moreover, this method can help to focus research on those beach stretches with large shoreline changes where the use of better resolution methods can help to understand the processes taking place.

4.3 Sea level variations

Sea level changes due to the astronomical tide and storm surges cause horizontal movements of the instanta neous shoreline detected by satellites. The predicted tidal range for the Yucatan Peninsula is around 80 cm, and measured beach profiles suggest that the beach slope at the water line on the eastern side of the pier at Progreso is between 0.05 and 0.3 resulting in an estimated horizontal tidal shoreline excursion of between 16 and 2.6 m. This excursion is comparable with the pixel resolution of 10 m but may be detectable when a veraging shoreline changes over longshore stretches.

The DGPS measurements of the shoreline began at the eastern side of the pier and then moved to the western side and during this period the tide level was falling, with a predicted drop of around 19 cm between the start and end of the measurement period. To see whether this drop is detectable we have computed separate means and standard deviations of the differences between the measured and satellite-derived shorelines for the eastern and the western sides of the pier. For the eastern side, the resulting mean is +2.3 m with a standard deviation of 2.1 m whilst to the west the mean is -4.2 m with a standard deviation of 2.8 m. A positive mean indicates that the DGPS shoreline is landward of the satellite shoreline, so the drop in the mean from east to west is qualitatively consistent with a drop in sea level over the measurement period. However the magnitude of the difference is much greater than expected on the basis of the predicted drop in tide level; a 19 cm drop on a beach slope between 0.05 and 0.3 gives a difference of only 0.6 – 3.8 m, whilst the observed difference from east to west is 6.5 m. Interestingly however the measured vertical elevations of the DGPS survey also provide some independent evidence that the actual drop in mean water level was considerably larger than the tide prediction. Figure 3 shows a plot of the DGPS vertical elevation, corrected for atmospheric pressure variations, versus the predicted tide level. The rapid variations may represent fluctuations in the swash line but there is a longer term slope which fits a linear trend with a high correlation (r^2=0.8). However the slope of this trend is about three times greater than expected, suggesting a drop of sea level of around 40 cm; with atmospheric pressure effects included this increases to around 50 cm. The equivalent horizontal shoreline excursion would be between 1.6 and 10 m, thus spanning the observed difference between the means to the east and west of the pier.

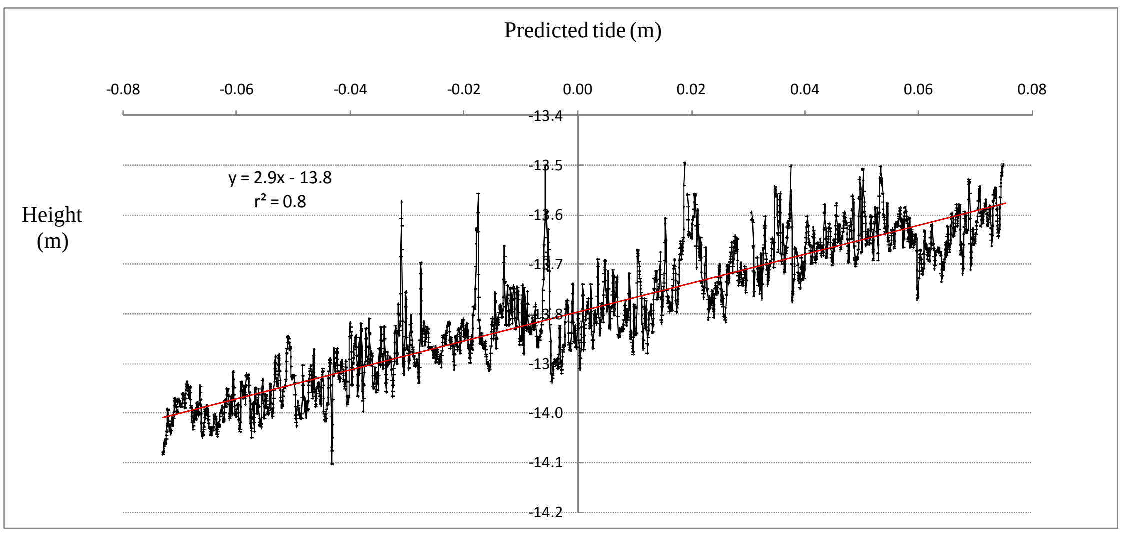

Figure 3. Predicted tide in meters in the horizontal axis and corrected height to a standard atmospheric pressure along the beach surveyed in Progreso, Mexico on September 9th 2008.

It is possible that this inferred sea level change during the measurement period was caused by a storm surge associated with the passage of Hurricane Ike across the Gulf of Mexico. Hurricane Ike was category 4 as it approached Cuba on 4th September but at the time of the field measurements on the 9th it was only category one and was growing again as it emerged across the Cuban coast, about 660 km away. At Progreso, a change in wind direction was observed, but no significant increase in wind speed or wave height was experienced. However it is possible that the associated storm surge could have affected the sea level at the shoreline. As a category 1 hurricane, the Saffir-Simpson scale suggests an associated surge level of only 1.2-1.5 m in the vicinity of the eye. However Hurricane Ike was unusually large, with an estimated diameter of up to 780 km, and as a result a storm surge of up to 6 m was experienced at its eventual landfall near Galveston, Texas (Berg, 2009). A drop in surge level of around 0.3 m as the Hurricane moved across the Gulf of Mexico during the measurement period may therefore be plausible. Note that the hurricane was no longer present by the time of the satellite image on 20th September 2008.

The conclusion is that surges on the Yucatan coast can create sea level changes significantly larger than tidal variations and may cause large horizontal excursions of the shoreline in extreme cases. Shorelines deri ved from satellite images taken during the close passage of large storms and hurricanes should therefore be interpreted with caution.

4.4 Comparison of satellite-extracted shorelines from different years.

In this section we describe the shoreline changed observed from satellite images from 2008, 2006 and 2004 (Table 2). The shorelines extracted from the 2004 and 2006 images compare well with the inferred shoreline locations from the beach profiles measured on the dates given in table 2.

Figure 4A-B shows the three different satellite-derived shorelines overlaid on the 2008 satellite image. There are differences of more than 40 m between 2004 and 2008 shoreline. It is possible to appreciate that along the whole beach the oldest shoreline is consistently seaward of the most recent one and the 2006 shoreline shows that the landward movement has been progressive over this period.

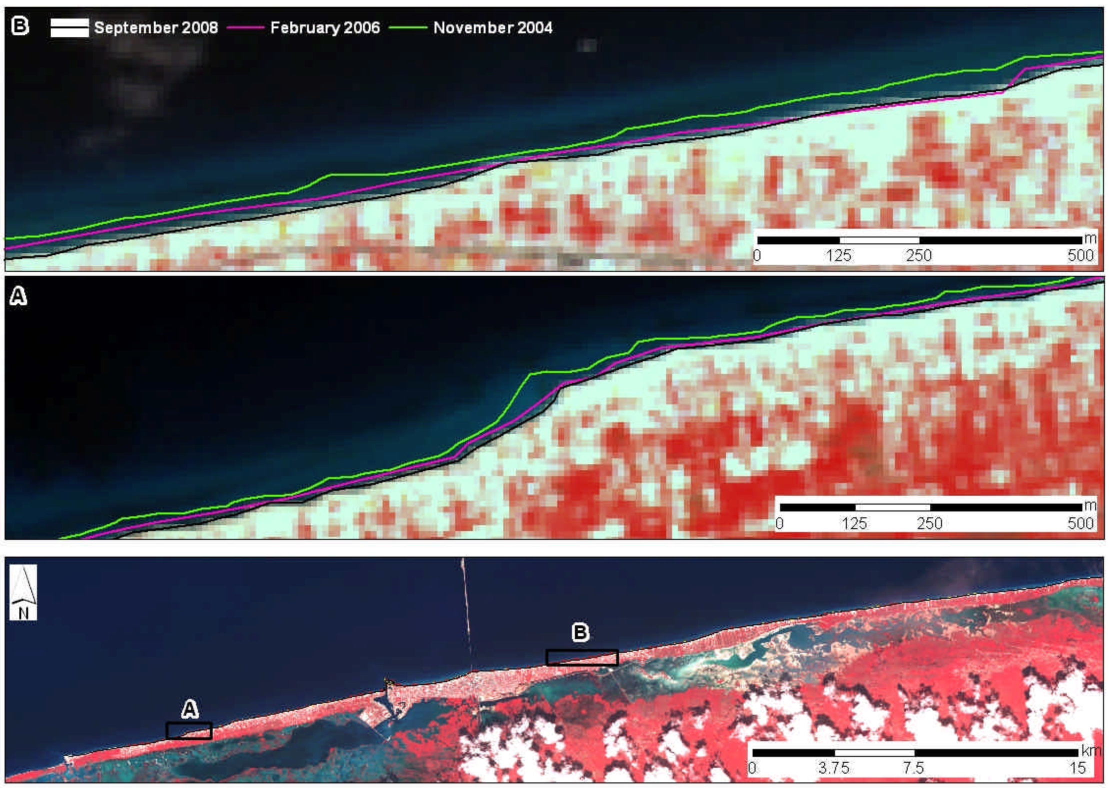

Figure 4. The upper images show a close up within the A and B squares shown in the lower image, showing three satellite-derived shorelines from 2004, 2006 and 2008.

Figure 4B show a close up of the region of the largest retreat of the shoreline position in the easterly beaches. This side of the pier shows the longest beach stretch of shoreline change for the whole study area. The difference between the 2004 to 2006 shorelines and 2008 shoreline is clear.

Figure 5 shows separately the mean differences between the measured 2008 shoreline and satellite-derived shorelines for the years 2008, 2006 and 2004 for the two sides of the pier. The landward trend of the shoreline location is evident for both sides and is much larger than the standard errors of the mean indicated by the error bars. As might be expected the standard deviations also decrease from 2004 to 2008, indicating a degree of alongshore variability in the rate of shoreline recession. Comparing the two sides of the pier, the east side shows a bigger net change and smaller standard deviation than the west side. This observation is consistent with a visual inspection of the images which suggests that the beach on the western side has a lower slope with more abundant sand held in shallow offshore bedforms. These results suggest that real changes in shoreline location can be detected using satellite imagery, and that the net trend during the studied period around Progreso is erosion.

The mean differences between the 2008 satellite-derived shoreline and the 2006 and 2004 shorelines have been calculated for the complete 50 km beach stretch of overlapping satellite shorelines. Between the 2008 and 2006 shoreline, the mean change of shoreline location is 9.2 m landwards with a standard deviation of 6.1 m, and the maximum difference is 37 m. This mean change in the shoreline position is similar to that observed for the 8 km stretch covered by the in situ measurement (Figure 5).

The difference in tide between the two images (2006-2008) is around 35 cm and hence cannot cause this magnitude of change in shoreline location. Moreover close to the dates of the image acquisitions tropical cyclones of strength capable of producing a change of the observed magnitude were not present.

Nevertheless, between 2006 and 2008 several tropical storms and hurricanes had taken place close to the Progreso beaches. During the 2006 Atlantic Hurricane Season 10 tropical cyclones occurred (NHC, 2006). The tropical storm Alberto was particularly close to Yucatan beaches. During the 2007 Atlantic Hurricane season, 17 tropical cyclones occurred, with two tropical cyclones in close proximity, Olga and Erin, and Hurricane Dean crossed the Peninsula in August (NHC, 2007). In 2008 10 tropical cyclones occurred before the satellite acquisition, Hurricane Dolly crossed very close to the Progreso beaches (NHC, 2008). All these tropical cyclones events were likely to have had an impact on the wave conditions and on the Yucatan beaches.

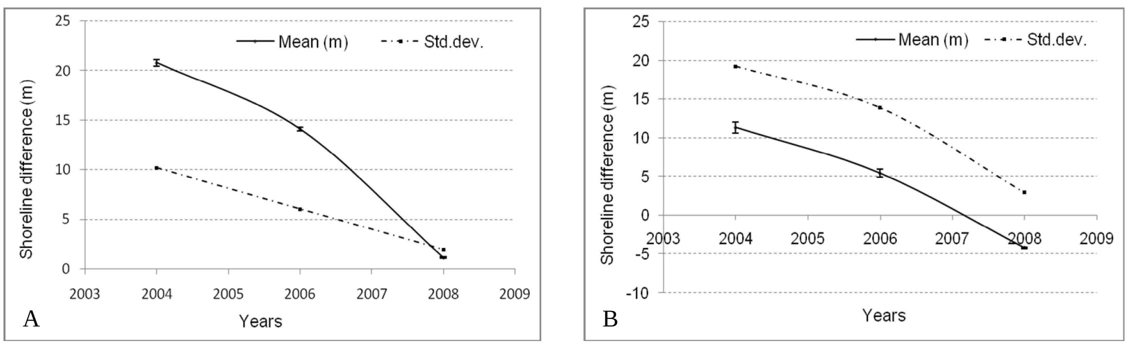

Figure 5. Mean differences (with error bars showing s.e. of the means) and standard deviations between the satellite-derived shoreline and the in situ shoreline from 2008 for the east side of the pier (A) and the west side of the pier (B).

Overall the difference between the mean 2008 and 2004 shorelines shows a landwards movement of 16.2 m and a standard deviation of 10.3 m, with a maximum difference of 56 m. The tide difference for the images is around 20 cm and the absence of tropical cyclones close to the date of the image acquisition gives some confidence that the shoreline change detected through these images represents a real change. In considering the storm conditions between 2008 and 2005, the hurricane season of 2005 ranks as the season with the highest Accumulated Cyclone Energy since 1899 (AOML-NOAA), with 28 tropical cyclones, some of which tracked close to the Yucatan peninsula (NHC, 2005). The strength of the 2005 hurricane season is likely to be a major contributor to the changes observed between 2004 and 2006.

It is instructive to look in more detail at locations which show the largest shoreline changes. The regions showing maximum shoreline differences between 2006 and 2008 coincide with the beach stretches that show maximum shoreline change from 2004 to 2008. This suggests that consistent local dynamics is taking place here, causing beach erosion. In addition, these sections coincide with regions of low coastal vegetation and the presence of coastal buildings, suggesting that the changes are related to human modifications. In contrast, beach stretches exhibiting less shoreline change generally have more vegetation cover and are far away from beach buildings.

Further work is needed using older images to explore whether the erosive trend can be detected over a longer period. We also plan to use numerical modelling to investigate the relative roles of tropical storms, winter northerly winds and beach management actions, in contributing to the longer term trends observed in the satellite images.

5. Conclusions

Shoreline identification from georeferenced SPOT satellite images using an unsupervised classification show excellent agreement with a visually estimated shoreline. The spectral behaviour between the water and the land are different and sharp enough to identify shoreline using an unsupervised classification. A DGPS survey of an 8 km section of shoreline taken within 11 days of a satellite image shows a mean difference between the ground and the satellite-derived shoreline of around -0.19 m and a standard deviation of 4 m, both smaller than the pixel size.

When comparing different satellite-derived shorelines, the current tide level, possible effects of storm surges and an estimate of the beach slope should be considered. The beach slope is required in order to assess the magnitude of any change in shoreline location due to differences in instantaneous water level.

Comparisons between satellite-derived shorelines for 2004, 2006 and 2008 strongly suggest that this method can be useful to explore changes over long periods of time in places without suitable in situ data. The fact that the biggest shoreline changes were consistently observed at the same locations also indicates that the method can be useful to focus research on those beach stretches most at risk.

Further work will include the use of numerical models to study the relative contributions of tropical storms, winter conditions and human impacts such as dune removal and the establishment of groynes, to the longer term overall shoreline changes observed by satellites. We will also use additional images, including older, lower resolution, satellite images to assess whether recent trends reflect longer term changes, with the overall aim of understanding which factors are the most important drivers of shoreline change in the Yucatan peninsula.

Acknowledgements

We wish to thank Dr. Ismael Mariño for providing the beach profiles for the Progreso beach and the facilities provided to do fieldwork. Thanks are also extended to CONACYT for the scholarship provided, to CONAFOR for providing the 2004 and 2006 SPOT images and to Mariana Gonzalez Leija for her valuable help in fieldwork.

References

Addo, K. A., Walkden, M. & Mills, J. P., 2008. Detection, measurement and prediction of shoreline recession in Accra, Ghana. *ISPRS Journal of Photogrammetry & Remote Sensing*, 63: 543-558.

Atlantic Oceanographic and Meteorological Laboratory- National Oceanic and Atmospheric Administration (AOML-NOAA). Hurricane Research Division. http://www.aoml.noaa.gov/hrd/tcfaq/E11.html.

Alvarez, E., Rubio, R. & H, Ricalde, 2007. Beach restoration with geotextile tubes as submerged breakwaters in Yucatan, Mexico. *Geotextiles and Geomembranes*, 25: 233-241.

Berg, R. 2009. National Hurricane Center. http://www.nhc.noaa.gov/2008atlan.shtml.

Capurro-Filograsso, L., J. Herrera Silveira, J. Euan Avila, I. Mariño Tapia, C. Enriquez Ortiz, V. Castillo, J. Acosta, 2006., Coastal Evolution of the Western Littoral of the Yucatan Peninsula-Erosion and Water Quality. Final report. CONACYT and World Bank funded research project.

Chu, Z. X., X. G. Sun, S. K. Zhai, K.H. Xu, 2006. Changing pattern of accretion/erosion of the modern Yellow River (Huanghe) subaerial delta, China: Based on remote sensing images. *Marine Geology*, 227:13-30.

De Wolf, P., D. Fransaer, J. Van Sieleghem, R. Houthuys, 1994. Morphological Trends of the Belgian Coast shown by 10 Years of Remote-Sensing based Surveying. *Coastal Zone Proceedings*. 245-257, NO, Louisiana.

Dinesh Kumar, P. K., G. Gopinath, C. M. Laluraj, P. Seralathan, D. Mitra, 2007. Change Detection Studies of Sagar Island, India, using Indian Remote Sensing Satellite 1C Linear Imaging Self-Scan Sensor III Data. *Journal of Coastal Research*, 23(6):1498-1502.

Dyer, K.R., 1986. *Coastal and Estuarine Sediment Dynamics*. Wiley –Interscience.

Lafon, V., Froidefond, J. M., Lahet, F. & P. Castaing, 2002. SPOT shallow water bathymetry of a moderately turbid tidal inlet based on field measurments. *Remote Sensing of Environment*, 81: 136-148.

Lafon, V., D. De Melo Apoluceno, H. Dupuis, D. Michel, H. Howa, J. M. Froidefond, 2004. Morphodynamics of nearshore rhythmic sandbars in a mixed-energy environment (SW France): Mapping beach changes using visible satellite imagery. *Estuarine, Coastal and Shelf Science*, 61:289-299.

Liu, H. & K.C.Jezek., 2004. Automated extraction of coastline from satellite imagery by integrating Canny edge detection and locally adaptive thresholding methods. *International Journal of Remote Sensing*, 25(5): 937-958.

Magaña-Chuc, R. E., 2006., *Procesos Dinámicos de Erosión –Acreción en las costas de Chuburná Chelem, Yucatán.* Instituto Tecnológico de Campeche. CINVESTAV-IPN.

Meyer-Arendt, K. J., 1993. Shoreline Changes along the North Yucatán Coast. *Proceedings of the Eight Symposium on Coastal and Ocean Management Coastlines of the Gulf of Mexico*, 1993:103-117.

Morel, A., 1974. Optical properties of pure water and pure sea water. in Jerlov, N.G. and Steeman-Nielsen, E. eds. *Optical Aspects of Oceanography*. Academic Press.

National Hurricane Center, (NHC)., 2005. *2005 Atlantic Hurricane Season*. http://www.nhc.noaa.gov/2005atlan.shtml

National Hurricane Center, (NHC)., 2006. *2006 Atlantic Hurricane Season*. http://www.nhc.noaa.gov/2006atlan.shtml

National Hurricane Center, (NHC)., 2007. *2007 Atlantic Hurricane Season*. http://www.nhc.noaa.gov/2007atlan.shtml

National Hurricane Center, (NHC)., 2008. *2008 Atlantic Hurricane Season*. http://www.nhc.noaa.gov/2008atlan.shtml

Programa de Ordenamiento Ecológico del Territorio Costero del estado de Yucatán (POETCY) in press. Semarnat, Merida, Yucatan, Mexico.

Provost, J.-N., C.Collet, Rostaing, P., Pérez, P. & P. Bouthemy, 2004. Hierarchical Markovian segmentation of multispectral images for the reconstruction of water depths. *Computer Vision and Image Understanding*, 93:155-174.

Pugh, D., 2004. *Changing Sea Levels: Effects of Tides, Weather and Climate*. Cambridge: Cambridge University Press.

Theodoridis, S. and K. Koutroumbas., 2006. *Pattern recognition*. Third ed. Elsevier.

White, K. & H. M. El Asmar, 1999. Monitoring changing position of coastlines using Thematic Mapper Imagery, an example from the Nile Delta. *Geomorphology*, 29:93-105.